

Y. Trotsenko¹, Cand. Sc. (Eng.), Assoc. Prof., ORCID 0000-0001-9379-0061

T. Katsadze¹, Cand. Sc. (Eng.), Assoc. Prof., ORCID 0000-0002-8365-0046

M. Dixit², Assoc. Prof., ORCID 0000-0003-1959-7815

J. Peretyatko¹, Cand. Sc. (Eng.), Assoc. Prof., ORCID 0000-0003-1397-8078

¹National Technical University of Ukraine "Igor Sikorsky Kyiv Polytechnic Institute"

²Vishwaniketan Institute of Management Entrepreneurship and Engineering Technology

ELECTRICITY TRANSMISSION AND ENVIRONMENT: EFFECT OF WIND LOADS ON LIGHTNING SHIELDING PERFORMANCE OF OVERHEAD POWER LINES

In this paper the estimation of wind load effect on the lightning shielding performance of overhead power lines was performed. According to electro-geometrical model any phase conductor has horizontal exposure width where this conductor is not protected against lightning by the overhead ground wire. A typical double circuit 220 kV lattice power transmission line tower was considered. Obtained results demonstrate that in the presence of thundercloud in windy conditions unprotected distance of phase conductor may increase due to deflections of phase conductors. Geometric locations of the conductor attachment points on the suspension insulator string and the lower point of the conductor sagging were calculated in the range of wind pressure from 0 to 800 Pa. This allowed to determine the exposure width values of a 220 kV overhead power line upper phase conductor in the same range of wind pressure values. The results show that for a minimum lightning current of 3 kA, the unprotected distance increases by 4.323 times from 4.167 m to 18.013 m when the wind pressure increases from 0 to 800 Pa (from 0 to 36.140 m/s). For a minimum lightning current of 5 kA, the unprotected distance increases by 7.735 times from 2.825 m to 21.851 m when wind pressure and wind speed vary in the same range. Although the transmission line is reliably protected against lightning strikes with currents greater than 16 kA at wind pressure of up to 200 Pa (18.070 m/s), when the wind pressure increases from 300 Pa to 800 Pa (from 22.131 m/s to 36.140 m/s), the unprotected area increases from 4.752 m to 26.204 m. In Summary, the results show that the influence of wind load must be taken into account in the tasks of calculating lightning protection of overhead power lines. Further efforts should be focused on studying the lightning shielding performance of overhead power lines of higher voltage classes.

Keywords: lightning, shielding failure, overhead ground wire, wind load, electro-geometric model.

Introduction.

Overhead power lines as a part of the power system have direct contact and mutual influence with the environment. This means that power lines can both affect the environment and be affected by the environment. Effects on the environment due to the physical presence of power lines include [1-4]: deforestation along the route of the overhead power line; physical changes to wildlife habitat; birds collisions and electrocutions with overhead power lines; access issues; avoidance of overhead power lines by some animals due to noise effect and visual detection of corona discharge light; biological effects of electromagnetic fields on plants, animals and human beings. This is a list of the main, but not all, environmental problems. Among the examples of how the environment affects overhead power lines are strong winds causing conductors to break [5] and icing of power line wires and towers during winter storms also causing damages and electricity outages [6]. Phase conductors of overhead power lines are usually protected against lightning by one or two overhead ground wires (shield wires). Each shield wire has protected volume. In windy conditions, phase conductors can swing violently and gallop, and as a result, can go beyond the protected volume. Nowadays, for estimation of lightning shielding failure and possible lightning outages of overhead power lines, electro-geometric model and its various modifications are widely used [7-9]. According to [8, 10] observed number of lightning strokes to upper phase conductors of large-sized overhead transmission lines was larger than those obtained from computations based to conventional electro-geometric model. One of the explanations for this may be that some factors are not taken into account in the model.

Purpose of work:

The aim of the research is to study how wind loads can affect the lightning shielding performance of overhead power lines.

Research material.

The construction of overhead power lines determines the active influence of the surrounding environment on the operational characteristics of power transmission [11-13]. A change in surrounding air temperature, high-speed wind pressure and other atmospheric phenomena cause a change in the position of phase conductors and shield wire in air and, as a result, affect the lightning protection characteristics of the line.

A typical 220 kV power transmission line [14] was considered for calculating the position of the phase conductor and the shield wire in air. Aluminum conductor steel reinforced (ACSR) “ZEBRA” conductor was used, which physical and technical characteristics are given in Table 1.

Table 1. Physical and technical characteristics of ACSR “ZEBRA” conductor

Number and diameter of aluminum wires	54×3.18 mm
Number and diameter of steel wires	7×3.18 mm
Sectional area of aluminum part of wire	428.88 mm ²
Total sectional area	484.48 mm ²
Mass of conductor	1630.0 kg/km
Modulus of elasticity	73.2 GPa
Coefficient of linear thermal expansion	19.91×10 ⁻⁶ K ⁻¹

The shield wire is fixed on a double circuit self-supported lattice transmission line tower with a total height of 37.115 m. A transmission line tower has two sets of three phases. Phase conductors on the tower are fixed in three tiers, the height of the cross-arm of the lower tier is 17.22 m; of the upper tier is 29.17 m. The length of the cross-arm of the upper tier is 4.2 m. The conductor is fixed on insulator strings with a length of 2.879 m; the weight of the insulating suspension is 150 kg. A shield wire with an integrated optical fiber cable OPGW-2 is used for lightning protection of the line. The calculation was performed for an overall span length of 350 m and minimum ground clearance of 7.25 m.

The calculation of the position of the conductor in air was performed for the maximum possible (overall) sag that is illustrated in Fig. 1, showing the position of the lower tier conductor.

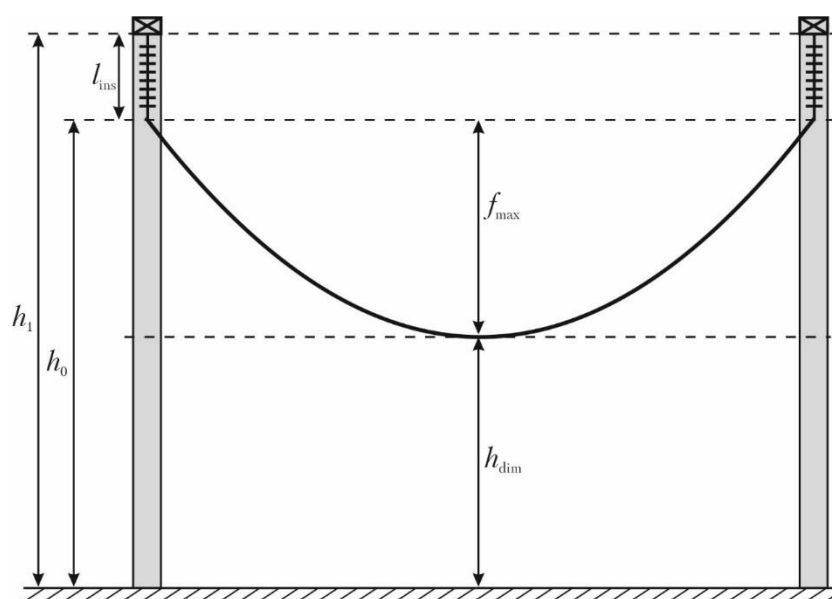


Figure 1 – Determining the sag of the lower phase conductor.

In Fig. 1, the following designations are used: h_1 is the height of the lower cross-arm above the ground level; h_0 is the height of fixing the lower tier conductor above the ground level; l_{ins} is the length of the suspension insulator string; h_{dim} is the ground clearance; f_{max} is the maximum possible (overall) sag of conductor. For the above transmission tower the sag is defined as:

$$f_{max} = h_1 - l_{ins} - h_{dim} = 7.091 \text{ m.} \quad (1)$$

The determination of the shield wire sagging is illustrated in Fig. 2, showing the position of the upper tier conductor and the shield wire that serves for lightning protection.

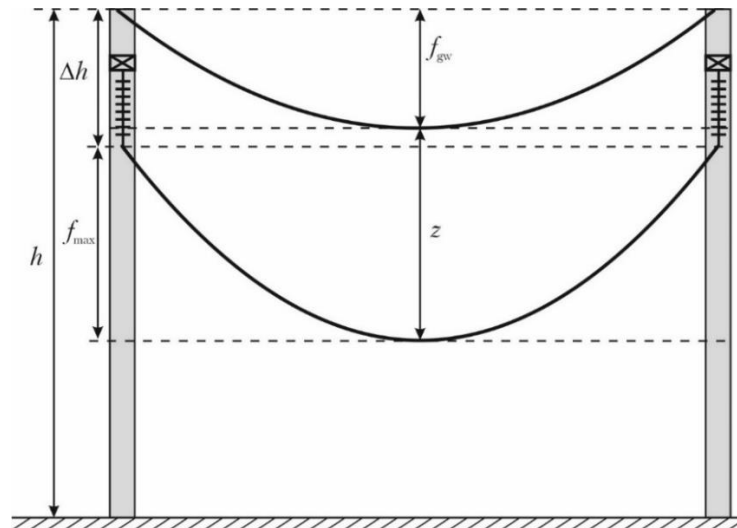


Figure 2 – Determining the sag of the shield wire.

In Fig. 2: h is the total height of the transmission line tower (the height of the shield wire attachment); Δh is the difference in height of fixing the shield wire and the upper tier phase conductor; f_{max} is the maximum possible (overall) sag of conductor; f_{gw} is the shield wire sag; z is the normalized vertical distance between the shield wire and the phase conductor in the middle of the span.

Linear interpolation of normalized values for a 350 m span of a 220 kV line allows to determine that vertical distance between the phase conductor and the shield wire in the middle of the span is 6.25 m.

Geometrical relationships according to Fig. 2 allow to calculate the shield wire sag:

$$f_{gw} = f_{max} + h - h_3 - l_{ins} + z = 5.907 \text{ m}, \quad (2)$$

where: h_3 is the height of the upper cross-arm above the ground level.

Thus, the height of the location of the lower point of sagging of the overhead ground wire above the ground level is

$$y_{gw} = h - f_{gw} = 31.208 \text{ m}. \quad (3)$$

Under the wind pressure, the plane of the sagging conductor deviates from the vertical state, as shown below in Fig. 3, where the curve AOB belonging to the vertical plane $ABCD$ shows the position of the conductor due to the vertical load due to the self-weight of the conductor p_v in the non-deflected state. Under the wind pressure, that is, as a result of the action of the horizontal load p_h , the plane of the sagging conductor deviates by an angle φ and takes the position $ABC'D'$. The curve $A'O'B'$ of the conductor position in the deflected state belongs to this plane. In Fig. 3 p denotes the total load that the conductor experiences; f' is the conductor sagging on the deflected plane $ABC'D'$, Δ is the horizontal projection of the movement of the lower point of the conductor sagging in the span.

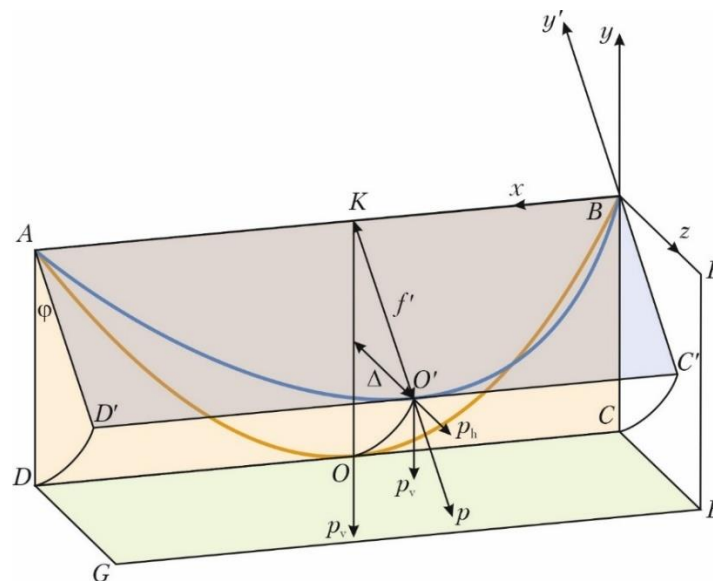


Figure 3 – Conductor deflection under wind pressure.

To calculate the position of the wire in the deflected state under the wind pressure, one will assume that the wind is directed perpendicular to the axis of the overhead power line, which causes the biggest deflection of the conductor. For spans up to 800 m long with sufficient accuracy, it can be assumed that the ratio of vertical and horizontal load at each point of the span is a constant value [11], which allows determining the deflection angle of the conductor sag using the expression:

$$\varphi = \arctan\left(\frac{p_h}{p_v}\right), \quad (4)$$

where: p_v, p_h denote single vertical and horizontal loads that the conductor experiences, respectively.

It was mentioned above that the vertical component of the load is determined by the conductor weight and is constant for all operating modes of power transmission:

$$p_v = g \cdot M_0 = 13.19 \text{ N/m}, \quad (5)$$

where: M_0 is the conductor weight per unit length, kg/m.

The horizontal component of the load is caused by wind pressure and is determined by the expression [11-13]:

$$p_h = C_x \cdot W \cdot \alpha \cdot d, \quad (6)$$

where: C_x is the aerodynamic coefficient (aerodynamic drag coefficient), which is equal to 1.1 for a conductor with a diameter of more than 20 mm [11]; W is high-speed wind pressure; $\alpha = 1.7 - 0.3 \cdot \log(W)$ is the coefficient of unevenness of wind gusts (not more than 1); d is the diameter of the conductor.

The corresponding total load that the conductor experiences due to its own weight and wind pressure is determined by the expression:

$$p_\Sigma = \sqrt{p_v^2 + p_h^2}. \quad (7)$$

The study of the conductor position in the span was carried out in the range of values of high-speed wind pressure from 0 to 800 Pa, where the upper limit of 800 Pa is determined by the design value of the maximum wind pressure of the studied power transmission.

Horizontal movement of the lower point of conductor sagging under wind pressure, according to the diagram in Fig. 3 is defined by the expression:

$$\Delta = f' \cdot \sin(\varphi), \quad (8)$$

where: f' is the conductor sagging on the deflected plane.

The latter value can be determined by solving the cubic equation of the state of the wire in the span, written in the following form [11]:

$$\frac{\gamma \cdot l^2}{8 \cdot f} - \frac{8}{3} \cdot \frac{E \cdot f^2}{l^2} = \frac{\gamma_0 \cdot l^2}{8 \cdot f_0} - \frac{8}{3} \cdot \frac{E \cdot f_0^2}{l^2} - \alpha \cdot E(t - t_0), \quad (9)$$

where: E is the modulus of elasticity of the conductor; α is the coefficient of linear thermal expansion of the conductor; γ is the specific load experienced by the conductor; t is the temperature; l is the span length; the index "0" indicates the parameters of the initial mode of average annual temperatures.

Solving equation (9) by the Cardano method allows one to determine the dependence of the conductor sag in the deflected plane due to the wind pressure, which is shown in Fig. 4.

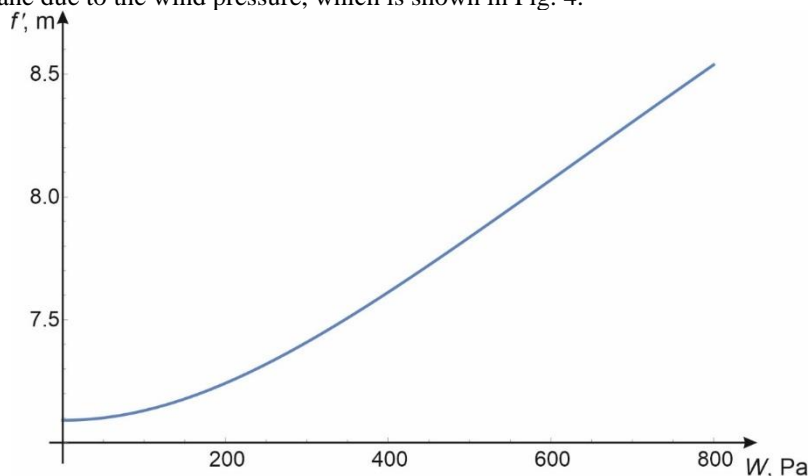


Figure 4 – Dependence of the conductor sag in the deflected plane due to the wind pressure.

Under the wind pressure, there is also a deflection from the vertical state of the suspension insulator string, as shown in Fig. 5.

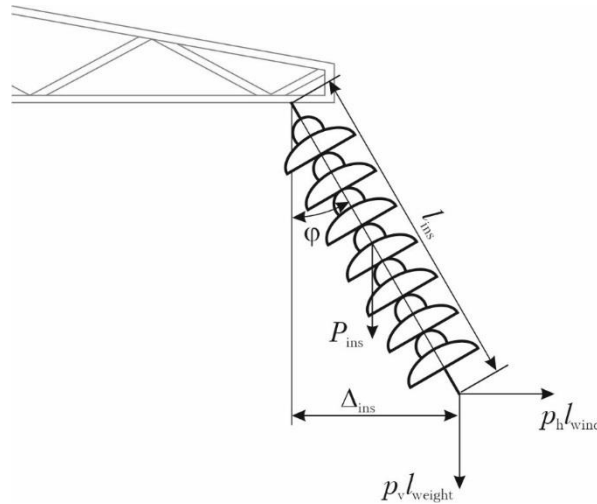


Figure 5 – Deflection of the suspension insulator string from the vertical state due to wind pressure

In Fig. 5: l_{ins} is the length of the suspension insulator string; P_{ins} is the concentrated load from the self-weight of the insulator string, applied in the center of mass (in the middle of the insulator string); p_v , p_h are vertical and horizontal load per unit length of the conductor, respectively; l_{weight} is the length of the weight span (the distance between the lower points of conductor sagging in the spans adjacent to the transmission line tower); l_{wind} is the length of the wind span (the distance between the centers of the spans adjacent to the transmission line tower); φ_{ins} is the deflection angle of the suspension insulator string from the vertical position; Δ_{ins} is the horizontal projection of the suspension insulator string in the deflected state.

To determine the position of the suspension insulator string in the deflected state, one will use the equation of the balance of moments of forces relative to the point of attachment of the insulating suspension to the cross-arm of the tower:

$$p_h \cdot l_{wind} \cdot \sqrt{l_{ins}^2 - \Delta_{ins}^2} - p_v \cdot l_{weight} \cdot \Delta_{ins} - g \cdot M_{ins} \cdot \frac{\Delta_{ins}}{2} = 0, \quad (10)$$

where: M_{ins} is the weight of suspension insulator string.

It follows from expression (10) that:

$$\Delta_{ins} = \frac{2 \cdot p_h \cdot l_{wind} \cdot l_{ins}}{\sqrt{4 \cdot p_v^2 \cdot l_{weight}^2 + 4 \cdot p_h^2 \cdot l_{wind}^2 + 4 \cdot p_v \cdot l_{weight} \cdot g \cdot M_{ins} + (g \cdot M_{ins})^2}}. \quad (11)$$

Note that in the absence of information about adjacent spans for a transmission line on flat terrain, it can be assumed with sufficient accuracy that the lengths of weight and wind spans are equal to the actual transmission line span: $l_{weight} = l_{wind} = l = 350$ m.

The deflection angle of the suspension insulator string from the vertical state, in turn, is determined by the expression:

$$\varphi_{ins} = \arcsin\left(\frac{\Delta_{ins}}{l_{ins}}\right). \quad (12)$$

Fig. 6 depicts the dependence of the deflection angles of the conductor sag plane (curve 1) and the suspension insulator string (curve 2) from the vertical state under the influence of wind load.

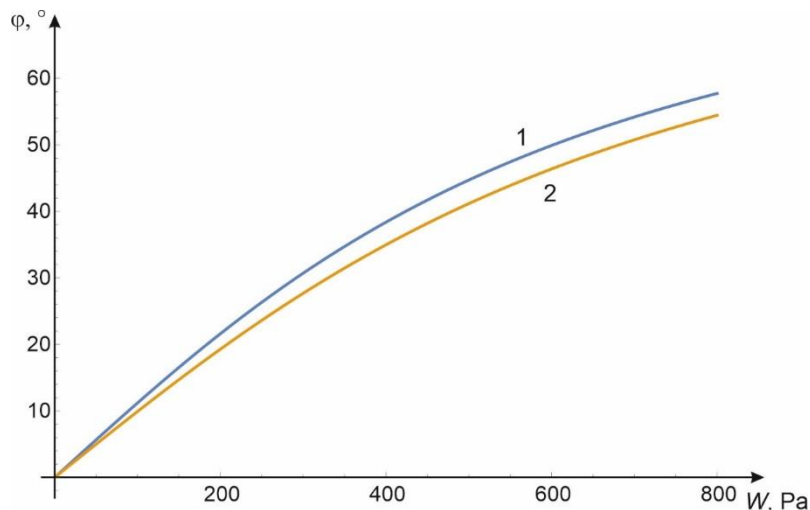


Figure 6 – Deflection angles of the conductor sag plane (curve 1) and the suspension insulator string (curve 2) from the vertical state under the influence of wind load

The coordinates of the lower point of conductor sag in the middle of the span in the coordinate system formed by the tower axis and the ground surface perpendicular to the transmission line axis are determined by the expressions (13) and (14):

$$x_c = x_3 + \Delta_{ins} + f_{max} \cdot \sin(\varphi), \quad (13)$$

$$y_c = h_3 - l_{ins} \cdot \cos(\varphi_{ins}) - f_{max} \cdot \cos(\varphi), \quad (14)$$

where: h_3 is the height of the upper (third) cross-arm above the ground level; x_3 – horizontal distance to point of attachment of the suspension insulator string to the upper cross-arm; f_{max} is the maximum possible (overall) sag of conductor; φ is the deflection angle of the sagging conductor plane from the vertical plane; l_{ins} is the length of the suspension insulator string; Δ_{ins} is the horizontal projection of the suspension insulator string in the deflected state; φ_{ins} is the deflection angle of the suspension insulator string.

Fig. 7 shows the geometric locations of the conductor attachment points on the suspension insulator string (curve 1) and the lower point of the conductor sagging (curve 2) in the range of wind pressure from 0 to 800 Pa.

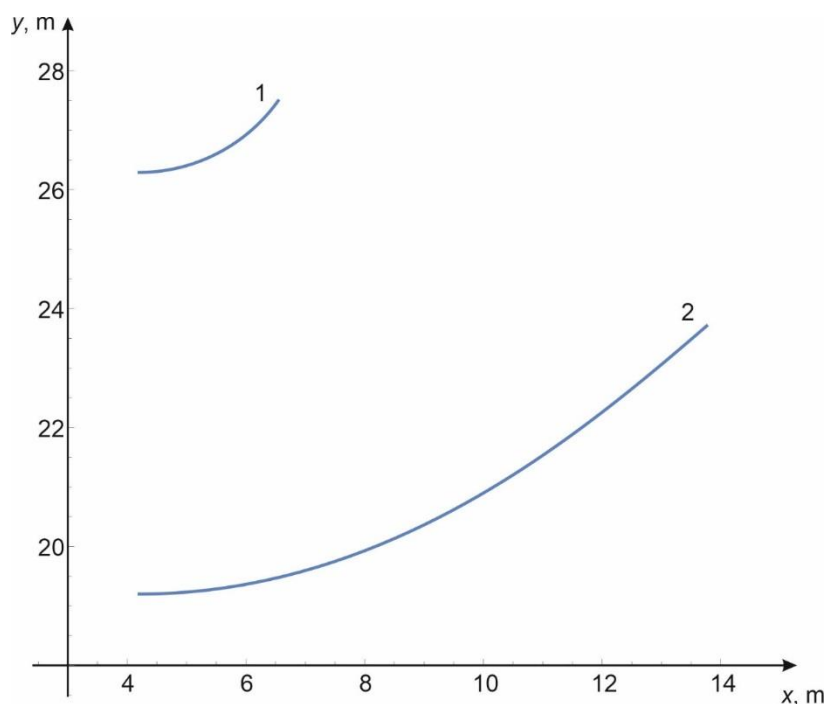


Figure 7 – Moving the attachment point and the lower point of the sagging conductor under the wind pressure

Table 2 contains information on the calculated values of the conductor position in air in the range of wind pressure values from 0 to 800 Pa with an increment of 100 Pa. The calculation procedure was performed through above steps (1)-(14).

Table 2 Calculated position of the upper phase conductor under wind pressure

Wind pressure, Pa	Wind speed, m/s	Deflection angle of suspension insulator string, degree	Deflection angle of sagging conductor plane, degree	Coordinates of lower point of conductor sagging, m	
				x_c	y_c
0	0	0	0	4.200	19.200
100	12.777	9.9	11.2	6.080	19.378
200	18.070	19.3	21.6	7.816	19.859
300	22.131	27.7	30.7	9.320	20.523
400	25.555	34.9	38.4	10.548	21.251
500	28.571	41.2	44.7	11.607	21.962
600	31.298	46.4	49.9	12.456	22.616
700	33.806	50.7	54.2	13.163	23.198
800	36.140	54.4	57.7	13.761	23.709

Traditional electro-geometric model is based on a striking distance approach [15]. The striking distance of the lightning flash is used to determine the magnitude of prospective stroke current that can bypass the overhead ground wire and hit the phase conductor:

$$r_c = 10 \cdot I^{0.65}, \tag{15}$$

where: r_c is the striking distance to phase conductor; I is the lightning current magnitude. In this article the striking distances to the overhead ground wire and to the phase conductor are assumed to be equal.

Fig. 8 below shows lightning shielding failure mechanism of studied 220 kV overhead transmission line according to traditional electro-geometric model. In Fig. 8-a the striking distances are used for visualization of unprotected area [15] and in Fig. 8-b the rolling sphere method is used [16]. The dotted lines in the illustrations show the sagging of the overhead ground wire and upper phase conductor.

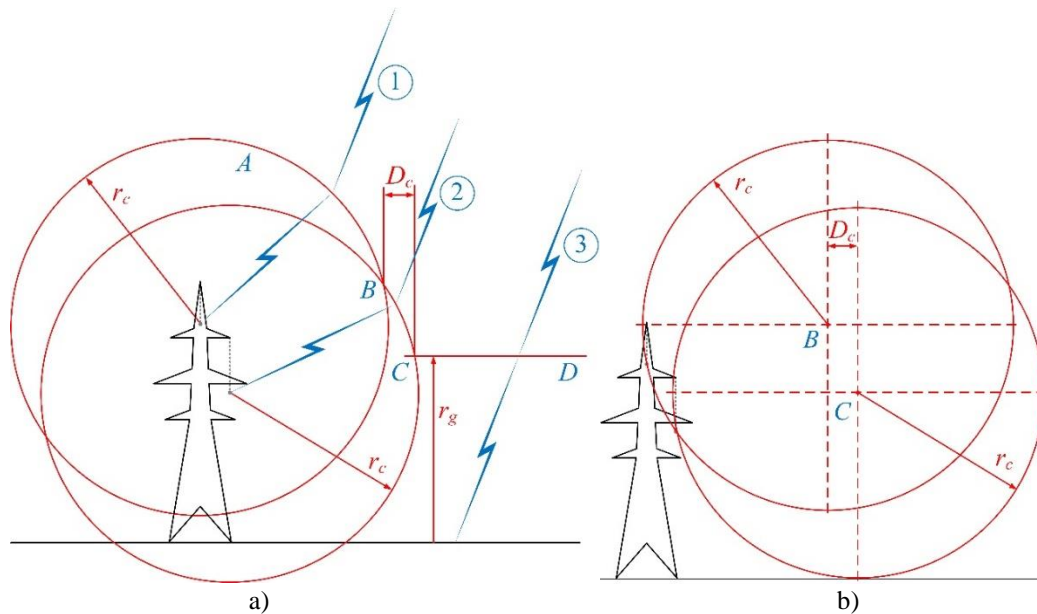


Figure 8 – Determining unprotected distance of phase conductor under absence of wind load: a) applying striking distance approach; b) applying rolling sphere method

In Fig. 8: r_c means the striking distances to the overhead ground wire, as well as to the phase conductor; r_g is the striking distance to the ground; D_c is the horizontal exposure width of the phase conductor, meaning the area unprotected by the shield wire.

Fig. 8-a, as well as Fig. 9 below show three cloud-to-ground flashes denoted by numbers 1, 2 and 3 propagating from thundercloud toward the overhead power line. All three flashes are of the equal lightning current peak value. According to electro-geometrical model concept, first lightning flash may hit only the overhead ground

wire, because anywhere on the arc AB , the distance to the phase conductor is too great. Third lightning flash may hit only the ground surface, because anywhere on the straight line CD , the distance to the phase conductor is also too great. Finally, only second lightning flash may strike the phase conductor, because anywhere on the arc BC , the distance to the phase conductor is less than distance to ground surface or to overhead ground wire. Horizontal exposure width D_c in Fig. 8-a and in Fig. 8-b is of equal length.

Wind pressure on the phase conductor changes the conductor self-weight per unit length horizontally in the direction of the air flow, causing the deflection of the conductor sagging from the vertical plane. The latter may affect efficiency of lightning protection of overhead power lines. Fig. 9 demonstrates how wind pressure on the phase conductor may increase the horizontal exposure distance D_c , unprotected by shield wire.

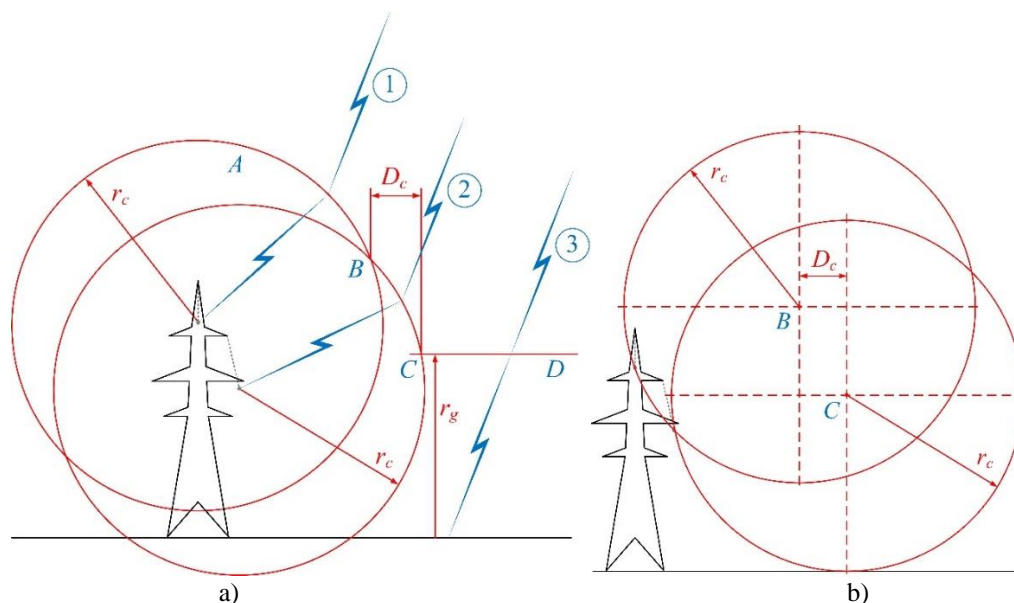


Figure 9 – Determining unprotected distance of phase conductor under presence of wind load:
 a) applying striking distance approach; b) applying rolling sphere method

Fig. 9 demonstrates that in the presence of thundercloud in windy conditions unprotected distance of phase conductor may increase due to deflections of phase conductors. Horizontal exposure width D_c in Fig. 9-a and in Fig. 9-b is of equal length. Table 3 contains information on the calculated values of the exposure width of upper phase conductor in the range of wind pressure values from 0 to 800 Pa with an increment of 100 Pa. In Table 3 minimum peak values of lightning current correspond to four lightning protection levels (LPL) [17]: 3 kA corresponds to LPL I, 5 kA corresponds to LPL II, 10 kA corresponds to LPL III and 16 kA corresponds to LPL IV.

Table 3. Calculated exposure width of the upper phase conductor under wind pressure

Wind pressure, Pa	Wind speed, m/s	Exposure width D_c (in meters) of phase conductor for minimum peak value of lightning current			
		3 kA	5 kA	10 kA	16 kA
0	0	4.167	2.825	effective shielding	effective shielding
100	12.777	6.262	5.399	0.574	effective shielding
200	18.070	8.489	8.295	4.705	effective shielding
300	22.131	10.649	11.219	9.005	4.752
400	25.555	12.575	13.915	13.057	10.055
500	28.571	14.313	16.393	16.825	15.010
600	31.298	15.762	18.505	20.077	19.304
700	33.806	16.983	20.310	22.879	23.014
800	36.140	18.013	21.851	25.284	26.204

In Table 3, the uncovered width D_c values were calculated through the following steps (16)-(19), according to [15].

$$\alpha_1 = \arcsin\left(\frac{r_g - y_c}{r_c}\right). \quad (16)$$

$$\alpha_2 = \arctan\left(\frac{x_c - x_{gw}}{y_{gw} - y_c}\right). \quad (17)$$

$$\alpha_3 = \arccos\left(\frac{\sqrt{(x_c - x_{gw})^2 + (y_{gw} - y_c)^2}}{2 \cdot r_c}\right). \quad (18)$$

$$D_c = r_c \cdot (\cos(\alpha_1) + \sin(\alpha_2 - \alpha_3)). \quad (19)$$

In (16)-(19): r_c is the striking distance to phase conductors; r_g is the striking distance to ground surface; x_c and y_c are the coordinates of a phase conductor; x_{gw} and y_{gw} are the coordinates of an overhead ground wire.

Conclusions.

In this paper the estimation of wind load effect on the lightning shielding performance of overhead power lines was performed. According to electro-geometrical model any phase conductor has horizontal exposure width where this conductor is not protected against lightning by the overhead ground wire. Obtained results demonstrate that in the presence of thundercloud in windy conditions unprotected distance of phase conductor may increase due to deflections of phase conductors. Geometric locations of the conductor attachment points on the suspension insulator string and the lower point of the conductor sagging were calculated in the range of wind pressure from 0 to 800 Pa. This allowed to determine the exposure width values of a 220 kV overhead power line upper phase conductor in the same range of wind pressure values. The results show that for a minimum lightning current of 3 kA, the unprotected distance increases by 4.323 times from 4.167 m to 18.013 m when the wind pressure increases from 0 to 800 Pa (from 0 to 36.140 m/s). For a minimum lightning current of 5 kA, the unprotected distance increases by 7.735 times from 2.825 m to 21.851 m when wind pressure and wind speed vary in the same range. Although the transmission line is reliably protected against lightning strikes with currents greater than 16 kA at wind pressure of up to 200 Pa (18.070 m/s), when the wind pressure increases from 300 Pa to 800 Pa (from 22.131 m/s to 36.140 m/s), the unprotected area increases from 4.752 m to 26.204 m. In Summary, the results show that the influence of wind load must be taken into account in the tasks of calculating lightning protection of overhead power lines. Further efforts should be focused on studying the lightning shielding performance of overhead power lines of higher voltage classes.

References

1. Gundula, S. B., Roel, M., Kjetil, B., Sigbjorn, S., Eivin, R. (2014), "The effects of power lines on ungulates and implications for power line routing and rights-of-way management", *International Journal of Biodiversity and Conservation*, Vol. 6, No. 9, pp. 647-662.
2. Tyler, N. J., Stokkan, K. A., Hogg, C. R., Nellemann, C., Vistnes, A. I. (2016), "Cryptic impact: Visual detection of corona light and avoidance of power lines by reindeer", *Wildlife Society Bulletin*, Vol. 40, No. 1, pp. 50-58, doi: 10.1002/wsb.620.
3. Manitoba Hydro (2010), "Fur, feathers, fins & transmission lines. How transmission lines and rights-of-way affect wildlife", pp. 1-90.
4. Trotsenko, Y., Nesterko, A., Peretyatko, Y., Dixit, M. (2022), "Mitigation of environmental impacts of electricity transmission: Effect of deciduous trees on electric field caused by overhead power lines", *Transactions of Kremenchuk Mykhailo Ostrohradskyi National University*, Issue 1 (132), pp. 203-211. doi: 10.32782/1995-0519.2022.1.27.
5. Nelson, O., Thomas, O. E. (2019), "Effect of wind environment on high voltage transmission lines span", *International Journal of Science and Engineering Applications*, Vol. 8, Issue 10, pp. 455-460, doi: 10.7753/IJSEA0810.1004.
6. Rossi, A., Jubayer, C., Koss, H., Arriaga, D., Hangan, H. (2020), "Combined effects of wind and atmospheric icing on overhead transmission lines", *Journal of Wind Engineering and Industrial Aerodynamics*, Vol. 204, Article 104271, doi: 10.1016/j.jweia.2020.104271.

7.Taniguchi, S., Tsuboi, T., Okabe, S., Nagarakı, Y., Takami, J., Ota, H. (2010), "Improved method of calculating lightning stroke rate to large-sized transmission lines based on electric geometry model", IEEE Transactions on Dielectrics and Electrical Insulation, Vol. 17, No. 1, pp. 53-62, doi: 10.1109/TDEI.2010.5412002.

8.Kern, A., Schelthoff, C., Mathieu M. (2011), "Calculation of interception efficiencies for air-terminations using a dynamic electro-geometrical model", 2011 International Symposium on Lightning Protection, pp. 25-30, doi: 10.1109/SIPDA.2011.6088439.

9.Trotsenko, Y., Nesterko, A., Dixit, M. (2021), "Analysis of approaches for estimating the lightning performance of overhead transmission lines", Transactions of Kremenchuk Mykhailo Ostrohradskyi National University, Issue 6 (131), pp. 116-121, doi: 10.30929/1995-0519.2021.6.116-121.

10.Taniguchi, S., Tsuboi, T., Okabe, S. (2009), "Observation results of lightning shielding for large-scale transmission lines", IEEE Transactions on Dielectrics and Electrical Insulation, Vol. 16, No. 2, pp. 552-559, doi: 10.1109/TDEI.2009.4815191.

11.Katsadze, T. L. (2012), "Fundamentals of mechanical calculations of overhead power lines: Textbook", Kyiv: Igor Sikorsky Kyiv Polytechnic Institute, ISBN 978-966-622-953-6.

12.Das, D. (2007), "Electrical power systems", New Delhi: New Age International, ISBN (13): 978-81-224-2515-4.

13.Grıgsby, L. L. (2007), "Electric power generation. Transmission and distribution", CRC Press, ISBN (13): 978-04-291-2973-5.

14.Central Electricity Authority (2018), "Compendium of tested tower designs for EHV transmission lines", Ministry of Power, Government of India, New Delhi, pp. 1-356.

15.LaForest, J. J. (1982), "Transmission line reference book (345 kV and above)", Electric Power Research Institute (EPRI), Palo Alto, CA, 2nd edition.

16.IEEE Std 1243-1997, "IEEE Guide for improving the lightning performance of transmission lines", pp. 1-44, doi: 10.1109/IEEESTD.1997.84660.

17.DEHN + SÖHNE (2014), "Lightning protection guide", 3rd updated edition, pp. 1-488, ISBN 978 3 9813770-1-9.

С.О. Троценко¹, канд.тех.наук, доцент, ORCID 0000-0001-9379-0061

Т.Л. Кацадзе¹, канд.тех.наук, доцент, ORCID 0000-0002-8365-0046

М. М. Діксіт², доцент, ORCID 0000-0003-1959-7815

Ю.В. Перегятко¹, канд.тех.наук, доцент, ORCID 0000-0003-1397-8078

¹Національний технічний університет України

«Київський політехнічний інститут імені Ігоря Сікорського»

²Інститут управління підприємництвом та інженерних технологій Вішванікетана

ПЕРЕДАЧА ЕЛЕКТРОЕНЕРГІЇ ТА НАВКОЛИШНЄ СЕРЕДОВИЩЕ: ВПЛИВ ВІТРОВОГО НАВАНТАЖЕННЯ НА ЕФЕКТИВНІСТЬ БЛИСКАВКОЗАХИСТУ ПОВІТРЯНИХ ЛІНІЙ ЕЛЕКТРОПЕРЕДАЧІ

У цій роботі проведено оцінку впливу вітрового навантаження на характеристики блискавкозахисту повітряних ліній електропередачі. Відповідно до електрогеометричної моделі будь-який фазний провідник має горизонтальну ділянку, де цей провідник не захищений від удару блискавки грозозахисним тросом. Розглянуто типову дволанцюгову гратчасту опору лінії електропередачі 220 кВ. Отримані результати показують, що за наявності грозової хмари у вітряних умовах ця незахищена ділянка фазного провідника може збільшуватися внаслідок відхилення фазних провідників. Геометричні положення точок кріплення провідників на підвісній гірлянді ізоляторів та нижню точку провисання провідника було розраховано в діапазоні тиску вітру від 0 до 800 Па. Це дозволило визначити значення ширини незахищеної ділянки верхньої фази лінії електропередачі 220 кВ у тому ж діапазоні значень тиску вітру. Результати показують, що для мінімального струму блискавки 3 кА незахищена відстань збільшується в 4,323 рази від 4,167 м до 18,013 м, коли тиск вітру зростає від 0 до 800 Па (від 0 до 36,140 м/с). Для мінімального струму блискавки 5 кА незахищена відстань збільшується в 7,735 разів з 2,825 м до 21,851 м, коли тиск і швидкість вітру змінюються в тому ж діапазоні. Хоча лінія електропередачі надійно захищена від ударів блискавки із струмами понад 16 кА при тиску вітру до 200 Па (18,070 м/с), при збільшенні тиску вітру від 300 Па до 800 Па (з 22,131 м/с до 36,140) м/с, незахищена відстань збільшується з 4,752 м до 26,204 м. Загалом, отримані результати показують, що вплив вітрового навантаження необхідно враховувати в задачах розрахунку блискавкозахисту повітряних ліній електропередачі. Подальші зусилля слід зосередити на вивченні характеристик блискавкозахисту повітряних ліній електропередачі вищих класів напруги.

Ключові слова: блискавка, відмова грозозахисту, грозозахисний трос, вітрове навантаження, електрогеометрична модель.

Надійшла 20.12.2022

Received 20.12.2022